

ELECTRON PARAMAGNETIC RESONANCE STUDIES OF $\text{TlIn}_{0.984}\text{Fe}_{0.016}\text{S}_2$ SOLID SOLUTION

**FAIK MIKAILZADE¹, SERDAR GÖKÇE¹, TOFIG G. MAMMADOV²,
ARZU I. NAJAFOV², MIRHASAN Yu. SEYIDOV¹**

¹ *Department of Physics, Gebze Technical University, Gebze, Kocaeli, 41400, Turkey*

² *Institute of Physics, National Academy of Sciences, Javid ave. 33, Baku, Azerbaijan*

E-mail: faik@gtu.edu.tr. Phone: +902626051311. Fax: +902626538490

The crystal structure studies and electron paramagnetic resonance (EPR) investigations of $\text{TlIn}_{1-x}\text{Fe}_x\text{S}_2$ with $x = 0.016$ have been performed. The observed energy dispersive X-ray (EDX) spectrum of $\text{TlIn}_{0.984}\text{Fe}_{0.016}\text{S}_2$ compound confirmed the presence of all the constituent elements in stoichiometric proportions. It has been concluded that the magnetic properties of $\text{TlIn}_{1-x}\text{Fe}_x\text{S}_2$ were induced by substituting trivalent iron atoms in the place of In^{3+} ion sites located at the center of $(\text{In}^{3+}\text{S}_4^{2-})$ structural units of TlInS_2 crystal. EPR study revealed an orthorhombic local symmetry around Fe^{3+} centers, which can be considered to originate crystal field arising from Tl ligands in the trigonal cavities surrounding Fe^{3+} transition metal ion. The rotational patterns of the EPR spectra showed the presence of two structurally equivalent Fe^{3+} centers localized at different sites of inter tetrahedron arrays of crystal structure.

Keywords: Magnetic semiconductors; electron paramagnetic resonance; fine structure splitting; crystal field.

1. INTRODUCTION

TlInS_2 belongs to a large family of thallium based ternary dichalcogenides having a general formula of $\text{Tl}^+(\text{M}^{3+}\text{X}_2^{2-})$, where M is trivalent cation of metal (In, Ga) and X is chalcogen anion (S, Se). TlInS_2 is a low - dimensional semiconducting material having layered crystal structure with monoclinic space group of $C_{2h}^6 - C2/c$ at room temperature [1, 2]. The structural, dielectric, optical, thermal properties and other experimental results obtained in recent decades are indicated that TlInS_2 single crystal is one of a few low - dimensional materials possessing a semiconducting and ferroelectric properties in the same compound [3-6]. On cooling from a room temperature, the temperature dependence of dielectric susceptibility, X - ray and neutron diffraction, and other characterizations of TlInS_2 have shown the pronounced anomalous behaviors typical for the structural phase transition to incommensurate and then to commensurate ferroelectric phases at the temperatures of about 216 K and 201 K respectively [7-10].

The reported crystal structure of TlInS_2 is composed from metal - chalcogen layers in the $a - b$ plane which is perpendicular to the pseudo c^* - axis ([001] direction) of the unit cell [7, 14]. The room temperature crystal structure of TlInS_2 is schematically shown in Fig. 1. As it is shown in Fig. 1, each layer consists of from In_4S_{10} tetrahedral complexes formed by corner - connected four InS_4 tetrahedrons which are bounded together via sharing Sulphur atoms at the corners. In this structure, two adjacent layers are stacked along c^* - axis and alternately turned away by a right angle forming trigonal prismatic voids where Tl^+ ions are located. The unit cell has two layers which are shifted a quarter of a unit along [110] and $[1\bar{1}0]$ directions and are separated by a van der Waals gap in between layer planes [1]. The angle between layer

plane and crystallographic $c -$ axis is about $\sim 100^\circ$ so that the crystal structure of TlInS_2 is formed in a monoclinic lattice. Additionally, since the crystal of TlInS_2 represents a layered - type structure, it tends to exhibit a polytype structure due to weak van der Waals forces. This leads to stacking of layers, which results in different lattice parameters c^* corresponding to various polytypes of the crystal structure [12, 13].

In this study, we use the isovalent substitution of In cationic sites of TlInS_2 with 1.6 % Fe^{3+} transition metals as a novel way to prepare dilute magnetic semiconductor on the base of thallium based ternary dichalcogenides. From EPR experiments on $\text{TlIn}_{1-x}\text{Fe}_x\text{S}_2$ it is concluded that Fe^{3+} ions really diluted into $(\text{In}^{3+}\text{S}_4^{2-})$ host units. In addition, the local site symmetry of Fe^{3+} ions was also examined from the analysis of ESR data in terms of crystal field theory.

2. EXPERIMENTAL METHODS

$\text{TlIn}_{1-x}\text{Fe}_x\text{S}_2$ (with $x = 0.016$) single crystals were prepared by using the modified Bridgman - Stockbarger technique. The samples in the form of thin plates with mirror - like surface used in this investigation were freshly cleaved along the (001) basal plane due to the existence of weak interlayer bonds. The elemental composition of as - prepared Fe - substituted TlInS_2 single crystal was determined by using scanning electron microscope *Philips XL 30 SFEQ* equipped with EDX spectrometer. EDX analysis was performed point to point on the surface of layer at 30kV. The penetration depth of the quality of the sample and crystal lattice parameters were investigated by using *Rigaku D - Max 2200 X - ray diffractometer* scanning from 20° to 90° with a rate 2° per minute. The diffractometer was operated at 40kV/20mA, using CuK_α radiation tube with wavelength $\sim 1.54 \text{ \AA}$.

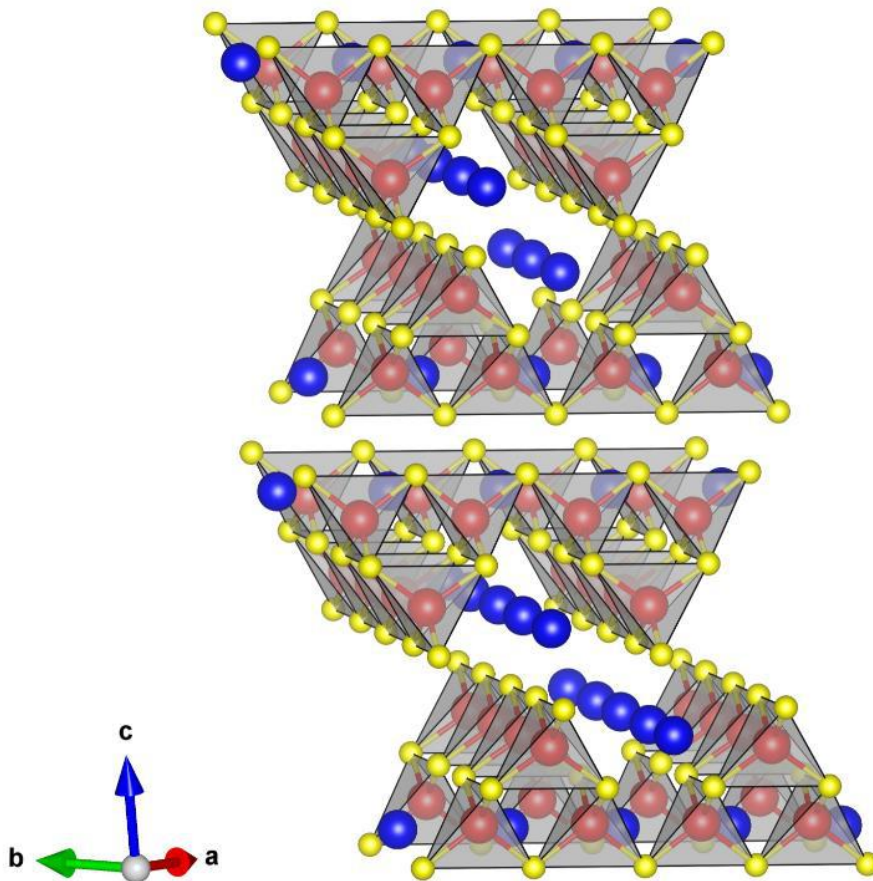


Fig. 1. Visualization of the crystal structure of TlInS_2 compound composed of InS_4 tetrahedrons based on the crystallographic data from reference [11]. The model is generated with VESTA code. The blue, red and yellow spheres represent Tl, In and S ions, respectively.

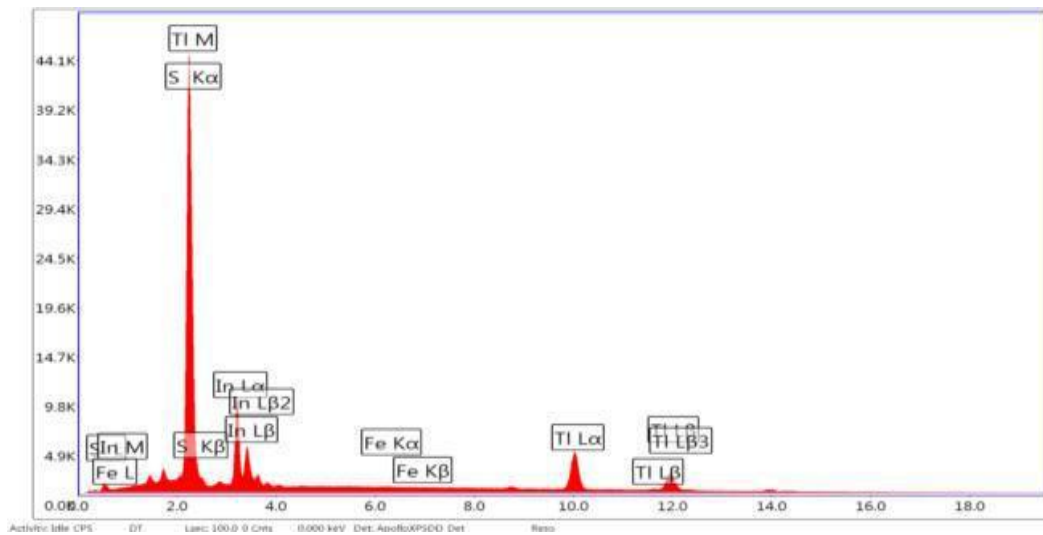


Fig. 2. The results of the EDX analysis of TlInS_2 .

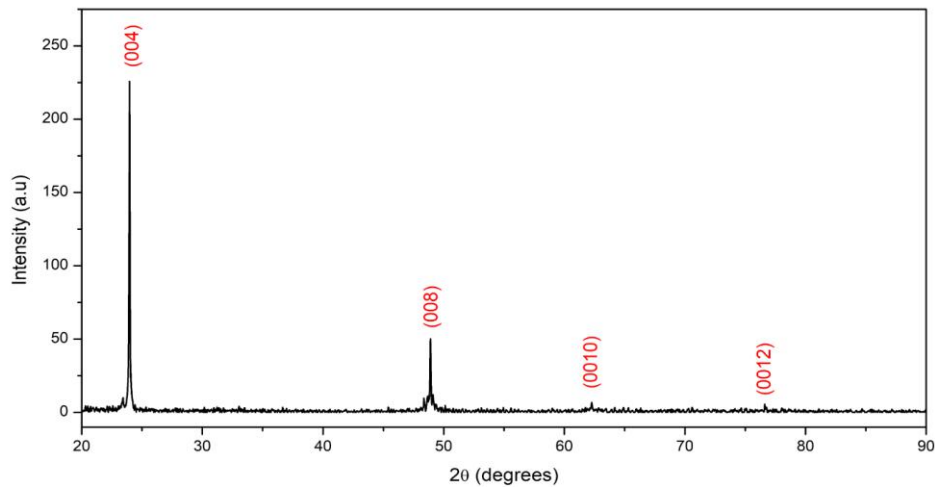


Fig. 3. XRD patterns of Fe³⁺ doped TlInS₂ crystal.

Room temperature EPR measurements were performed by applying a scanning magnetic field parallel (*in - plane* orientation) and perpendicular (*out - of - plane* orientation) to (001) or crystallographic *ab*-layer plane of sample by using X - Band (about ~ 9.2 GHz) JEOL JES - FA 300 spectrometer in the field range between 0 - 15 kOe. The field derivative of microwave power absorption (dP/dH) versus static magnetic field (H) was registered in steps of 10° degrees between 0 and 180°. During measurement process, frequency option could not be locked to the value of ~ 9.8 GHz for tuning resonance frequency in the EPR spectrometer. Therefore, the value of about ~ 9.2 GHz is chosen instead of ~ 9.8 GHz frequency. The crystal sample of rectangular form is placed on the quartz sample holder to perform angular dependence measurement of EPR spectra. The mirror-like surface face of sample is glued with vacuum grease to the bottom face of the quartz sample holder for performing in-plane measurement. Then, the static magnetic field is applied along the plane which is parallel to the mirror-like surface face of sample and the sample holder is rotated around surface normal to scan the static magnetic field in the layer plane. For out - of - plane measurement, the mirror - like surface face of sample is glued to the flat plane of the sample holder.

3. EXPERIMENTAL RESULTS

Fig. 2 shows the result of EDX analysis which confirms the presence of Tl, In, S and Fe elements in the TlInS₂ layered chalcogenide with substituted iron atoms, yielding a Tl/In/S stoichiometric ratio of 1:1:2. The weight ratios of components are 52 % of thallium, 30.08 % of indium, 17.68 % of sulfur and 0.23 % of iron. The atomic composition ratio of constituent elements Tl/In/S/Fe was detected as 23.74 : 24.44 : 51.43 : 0.39 at %, respectively. It is important to note that the sample has negligible amount of native impurities such as carbon, oxygen and silicon which are usually contained in undoped TlInS₂ crystal. This EDX studies showed that the examined sample has an insignificant deficit of Tl atoms and a little excess of S atoms with respect to the stoichiometric composition. It

is very important to note that no additional peaks corresponding to other impurities or contaminants are observed, which confirms the high purity of the prepared crystal. The substitution of Fe³⁺ ion into TlInS₂ with substitution of 0.39 % atomic percent does not practically influence atomic composition ratio of host compound. By substituting of 0.39 % Fe³⁺ ions for In³⁺ ones correspond to a molar ratio Fe³⁺/In³⁺ of about 1.6 %. It can be speculated from EDX studies that nanoscale chemical inhomogeneous and nonuniform spatial distribution of Fe³⁺/In³⁺ over compound are immanent for TlIn_{1-x}Fe_xS₂ solid solutions.

XRD pattern of Fe - substituted TlInS₂ taken single crystal in Bragg - Brentano geometry is shown in Fig. 3. It reveals that X - ray diffraction pattern contains high intensity (00*l*) reflections on the cleavage planes. The position of diffraction angles at ~ 23.95°, ~ 48.90°, ~ 62.26°, ~ 76.62° can be assigned to (004), (008), (0010), (0012) planes of the monoclinic crystal symmetry (C_{2h}⁶ - C2/c). From XRD spectra of this sample, it is noticed that (004) plane gives rise to high intensity and narrow peak while second high intensity is observed from (008) plane. (0010) and (0012) planes exhibit relatively low intensity peaks. The reflection positions of XRD pattern occurring from crystal layers is in accordance with the XRD results that reported previously in the literature [14-16]. It is clear that XRD pattern shows only 00*l* type reflections with even values of *l*. On the other hand, (00*l*) type reflections with odd values of *l* is not observed due to the space group C_{2h}⁶ [17]. The lattice parameter *c** determined from the angular position of (004) reflection for monoclinic crystal system is 14.83 Å. This value of *c** - parameter consistent with the data from [14,18]. Thus, Fe substitution doesn't affect the crystal structure of the pristine TlInS₂ single crystal. Whereas, heterogeneous distribution of the Fe³⁺ ions in TlInS₂ host should modify the local chemical bonding lengths in crystal due to an average radius difference between Fe³⁺ (~ 0.064 nm) and In³⁺ (~ 0.08 nm) ions [19].

In other words, the local lattice deformation effects arising from the Fe³⁺ ions substitution for In - sites with a larger iron concentration must be observed. Due to different local lattice distortions a slightly shift in the

XRD - peaks position in Fe – diluted TlInS_2 sample compared to the defect – free TlInS_2 compound should be observed. Additionally, the changes in the intensity of the diffraction peaks in $\text{TlIn}_{1-x}\text{Fe}_x\text{S}_2$ due to accumulation of excess (more than $x = 0.007$) Fe^{3+} ions outside of $(\text{In}^{3+}\text{S}_4^{2-})$ host lattice units should be expected. Most probably, the formation of iron precipitates into TlInS_2 crystal host due to low - solubility of Fe^{3+} magnetic ions were took place. However, to analysis our EPR experimental data we will use the approach where one indium atom was replaced by an iron ion as was documented during single - crystal growth experiments.

The experimental stack plots of X-band EPR spectra of Fe diluted TlInS_2 sample observed at room temperature for out-of-plane ($H \perp$ ‘ab-plane’) and in-plane ($H \parallel$ ‘ab-plane’) orientation are shown in Fig. 4 (a) and 4 (b), respectively. It can be seen that there is

strong anisotropy of EPR lines at out-of-plane orientation. Fig. 4 (c) and (d) demonstrate the rotation patterns of the resonance fields of Fe diluted TlInS_2 sample obtained for out-of-plane and in-plane orientation, respectively. The experimental data points are well fitted by simulated curves. The simulations of EPR rotation pattern were performed by using EasySpin software (version 5.2.35) [20]. It is concluded that the resonance lines originated from four structurally equivalent but two magnetically nonequivalent paramagnetic centers, whose symmetry axes are nearly perpendicular to each other [21]. The experimental and simulation results show that Fe^{3+} ions doped into TlInS_2 crystal substitute for the In^{3+} cations, which are localized in two crystallographically inequivalent sites represented by In(1) and In(2) [11]. The Fe^{3+} ions located at these sites will be hereafter denoted as Fe1 and Fe2 centers (as shown in Fig. 5).

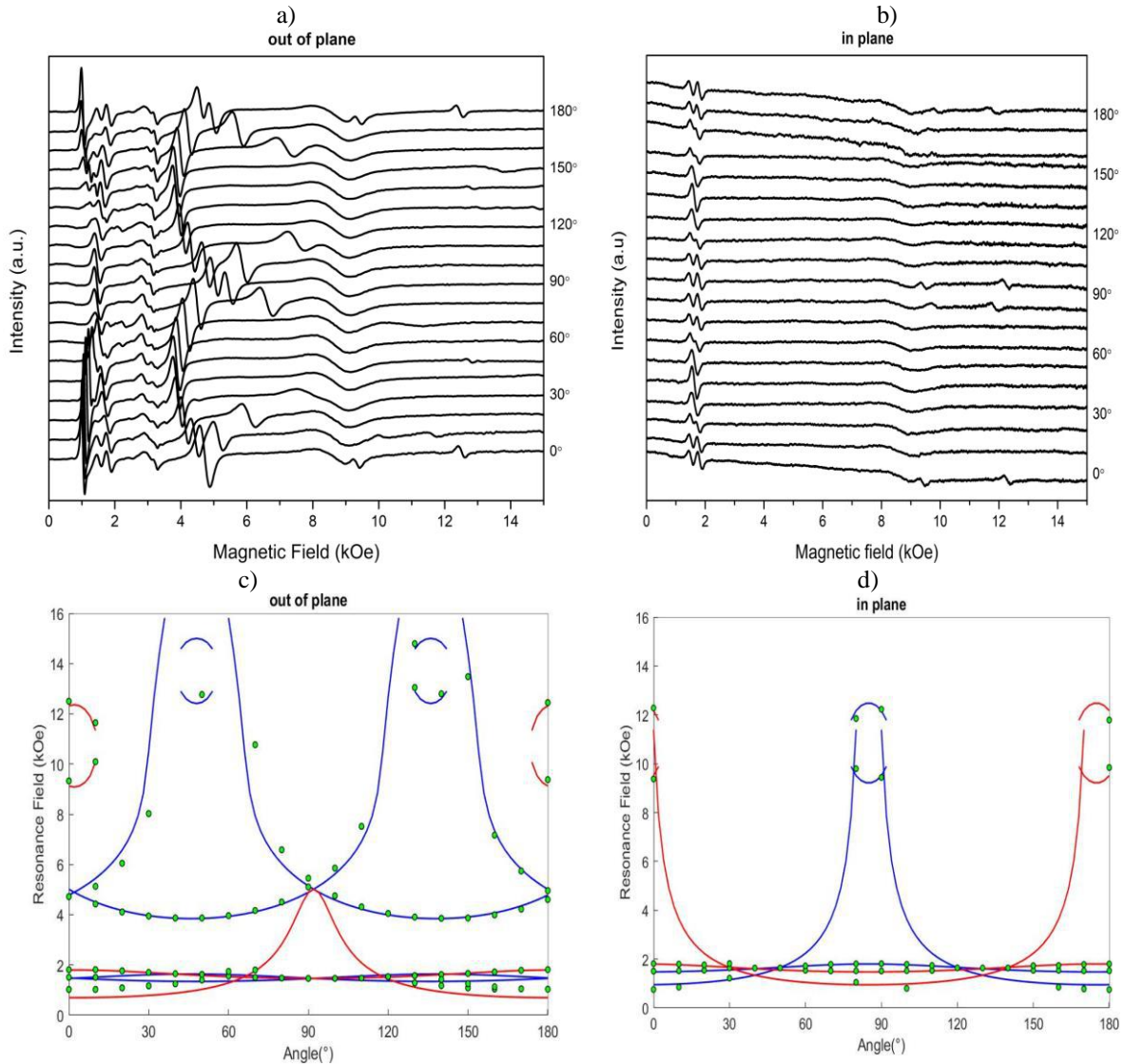


Fig. 4. EPR spectra obtained by scanning static magnetic field H (a) in \mathbf{ac}^* -plane (out-of-plane plane geometry) and (b) in \mathbf{ab} -plane (in-plane geometry) of Fe^{3+} diluted TlInS_2 crystal at room temperature. The rotational pattern of resonance fields for (c) out-of-plane and (d) in-plane orientation has been created by green dots read directly from the resonance field positions of EPR spectra. Blue and red lines indicate the simulated angular dependence of line positions for Fe1 and Fe2 centers, respectively.

In the iron diluted TlInS_2 fit model, the total spin Hamiltonian (H_T) should be defined to find zero field splitting (ZFS) factor of Fe^{3+} ion in the center of ($\text{Fe}^{3+}\text{S}_4^{2-}$) structural units that are surrounded by charges (ligand ions). The total spin Hamiltonian for orthorhombic symmetry can be expressed in terms of the extended Stevens operators [22]:

$$H_T = H_Z + H_{ZFS}^{ortho}$$

$$H_Z = \mu_B \mathbf{B} \cdot \mathbf{g} \cdot \mathbf{S}$$

$$H_{ZFS}^{ortho} = B_2^0 O_2^0 + B_2^2 O_2^2 + B_4^0 O_4^0 + B_4^2 O_4^2 + B_4^4 O_4^4 \quad (1)$$

where H_Z is electron Zeeman interaction, H_{ZFS}^{ortho} is orthorhombic part of ZFS Hamiltonian, μ_B is Bohr magneton, \mathbf{g} is the spectroscopic tensor, \mathbf{S} is electron spin operator, B_k^q ($k=2,4$; $q=0,2,4$) are fine structure parameters and O_k^q ($k=2,4$; $q=0,2,4$) are extended Steven operators. Where, the ZFS parameter of B_2^0 and B_2^2 are equivalent to the axial field splitting parameter $D/3$ and the rhombic splitting parameter E , respectively [23]. Fe^{3+} ion has electron configuration of $3d^5$ with ground state electron spin number $S=5/2$ (ground state ${}^6S_{5/2}$) [24]. The monoclinic part of ZFS Hamiltonian could be included to the total spin Hamiltonian when

the examined crystal possess monoclinic symmetry [25,11]. Since the unique axis (C_2) of monoclinic crystal is assigned to be along c^* -axis (Hermann-Mauguin symbol P112, see Crystal frame at [26]) in the EPR fitting procedure, the additional monoclinic term of ZFS spin Hamiltonian has been ignored.

The relative orientation between molecular frame (X_M, Y_M, Z_M) and crystal frame (X_{Cl}, Y_{Cl}, Z_{Cl}) for two paramagnetic centers localized at different sites of polyhedron structure are depicted in Fig. 5. The Euler angles (α, β, γ) specifying orientation between these frames are found to be $(0^\circ, 44^\circ, 0^\circ)$ and $(90^\circ, 44^\circ, 0^\circ)$ for Fe1 and Fe2 centers, respectively. The fitting result of ZFS parameters (B_2^2, B_2^0) and the rhombicity ratio $\lambda' = B_2^2/B_2^0$ for orthorhombic symmetry are presented Table 1. The found rhombicity values are seen to be close the previously reported values of TlInS_2 .

These results indicate that two type of centers which are structurally equivalent and orientationally different exist in the monoclinic unit cell of TlInS_2 with strong magnetic anisotropy and high rhombicity ratio. The cubic symmetry which is expected at In site of ($\text{In}^{3+}\text{S}_4^{2-}$) tetrahedron is lowered to the orthorhombic symmetry due to the effect of Tl atoms in the cavities between In_4S_{10} tetrahedral complexes.

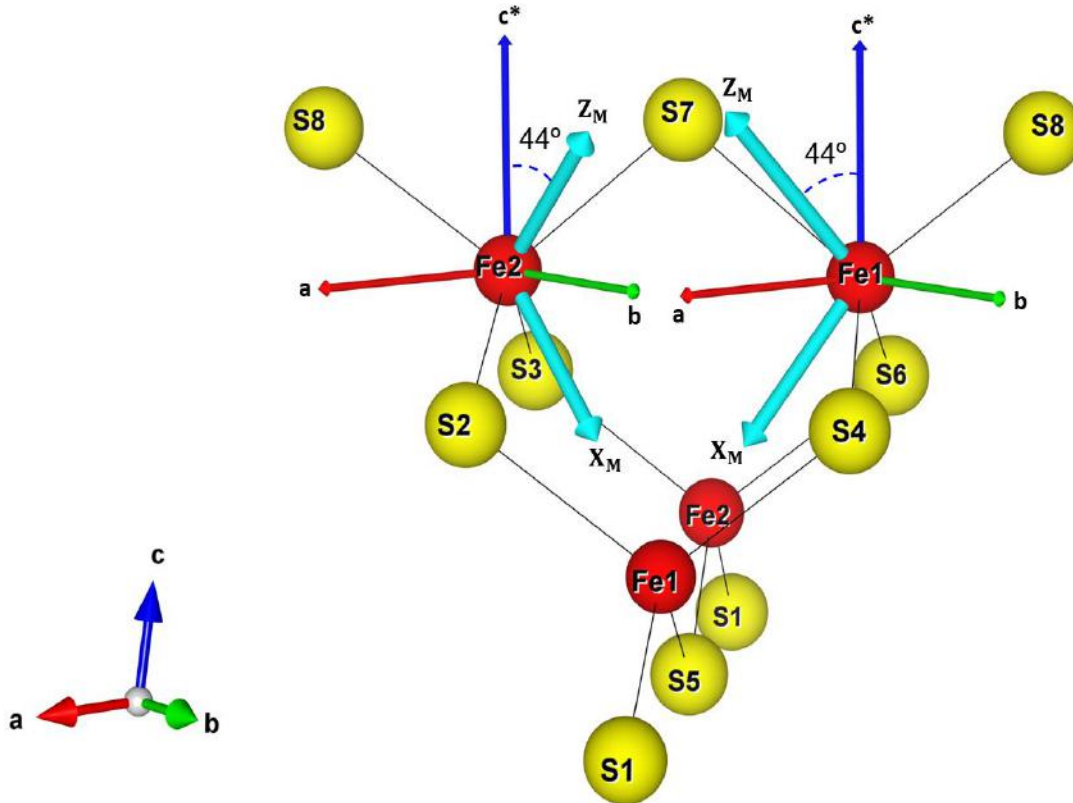


Fig. 5. Schematic representation of $\text{Fe}^{3+}\text{S}_4^{2-}$ polyhedron structure in $\text{TlIn}_{0.984}\text{Fe}_{0.016}\text{S}_2$ with molecular axes (X_M, Z_M , in light blue color) and crystallographic axes (a, b, c and modified c^*).

Table 1

The fitting results of ZFS parameters B_2^0 , B_2^2 and rhombicity ratio (λ') for $\text{TlIn}_{0.984}\text{Fe}_{0.016}\text{S}_2$ compound and previously reported sample. B_4^0 , B_4^2 , B_4^4 are approximately zero

Sample	B_2^0 (MHz/Oe)	B_2^2 (MHz/Oe)	$\sim\lambda'$
$\text{TlInS}_2 + \% 1.6 \text{ Fe}^{3+}$	6714/2375	4749/1680	0.707
$\text{TlInS}_2 + \% 0.7 \text{ Fe}^{3+}$ [21]	6785/2400	4806/1700	0.708

4. CONCLUSION

Thus, Fe diluted TlInS_2 layered semiconductor was prepared and characterized by using EDX and XRD analysis. EPR parameters of the Fe^{3+} ion center in the ternary layered TlInS_2 crystal at room temperature have been determined with the spin Hamiltonian. The crystal field coefficient of B_2^0 and B_2^2 is found to be 2375 and 1680 Gauss, respectively. The resultant ZFS crystal field parameters caused by Tl atoms are extracted. Thus, it is concluded that the Fe^{3+} ion centers substitute for the In sites located at the InS_4 tetrahedra

formed by S atoms. This EPR study reveals that the site symmetry of Fe^{3+} center in the monoclinic TlInS_2 crystal was determined to be orthorhombic. The orthorhombic local symmetry can be considered to originate crystal field arising from Tl ligands in the trigonal cavities surrounding Fe^{3+} metal ion. The angular dependence resonance lines show that the crystal lattice contain two structurally equivalent Fe^{3+} centers localized at different tetrahedron arrays of crystal structure.

- [1] W. Henkel, H.D. Hochheimer, C. Carlone, A. Werner, S. Ves. H.G. v. Schnering, High - pressure Raman study of the ternary chalcogenides TlGaS_2 , TlGaSe_2 , TlInS_2 , and TlInSe_2 , Phys. Rev. B. 26 (1982) 3211–3221. <https://doi.org/10.1103/physrevb.26.3211>.
- [2] D. Müller, H. Hahn. Untersuchungen über ternäre Chalkogenide. XXIV. Zur Struktur des TlGaSe_2 , Z. Anorg. Allg. Chem. 438 (1978) 258–272. <https://doi.org/10.1002/zaac.19784380128>.
- [3] D.F. McMorrow, R.A. Cowley, P.D. Hatton, J. Banys. The structure of the paraelectric and incommensurate phases of TlGaSe_2 , J. Phys.: Condens. Matter. 2 (1990) 3699–3712. <https://doi.org/10.1088/0953-8984/2/16/001>.
- [4] R.A. Aliev, K.R. Allakhverdiev, A.I. Baranov, N.R. Ivanov, R.M. Sardarly. Ferroelectric and structural phase transitions in crystals of TlInS_2 series, Fizika Tverdogo Tela, 26 (1984), 1271–1276
- [5] A.A. Volkov, Y.G. Goncharov, G.V. Kozlov, S.P. Lebedev, A.M. Prokhorov, R.A. Aliev, K.R. Allakhverdiev. Ferroelectric soft mode in the semiconductor crystal TlGaSe_2 , JETP Lett. 37 (1983) 517.
- [6] J.A. Kalomiros, N. Kalkan, M. Haniyas, A.N. Anagnostopoulos, K. Kambas. Optical and photoelectric properties of TlGaSe_2 layered crystals, Solid State Communications. 96 (1995) 601–607. [https://doi.org/10.1016/0038-1098\(95\)00423-8](https://doi.org/10.1016/0038-1098(95)00423-8).
- [7] S. Kashida, Y. Kobayashi. X-ray study of the incommensurate phase of TlInS_2 , J. Phys.: Condens. Matter. 11 (1999) 1027–1035. <https://doi.org/10.1088/0953-8984/11/4/010>.
- [8] K.R. Allakhverdiev, F.A. Mikailov, A.M. Kulibekov, N. Türetken. Thermal hysteresis and memory effects in TlInS_2 , Phase Transitions. 67 (1998) 457–465. <https://doi.org/10.1080/01411599808228753>.
- [9] F.A. Mikailov, E. Basaran, E. Şentürk. Improper and proper ferroelectric phase transitions in TlInS_2 layered crystal with incommensurate structure, J. Phys.: Condens. Matter. 13 (2001) 727–733. <https://doi.org/10.1088/0953-8984/13/4/318>.
- [10] F.A. Mikailov, E. Başaran, E. Şentürk. Time relaxation of metastable chaotic state in TlInS_2 , Solid State Communications. 122 (2002) 161–164. [https://doi.org/10.1016/s0038-1098\(02\)00113-8](https://doi.org/10.1016/s0038-1098(02)00113-8).
- [11] P. Gnutek, M. Açıköz, C. Rudowicz. Superposition model analysis of the zero-field splitting parameters of Fe^{3+} doped in TlInS_2 crystal – Low symmetry aspects, Optical Materials. 32 (2010) 1161–1169. <https://doi.org/10.1016/j.optmat.2010.03.024>.
- [12] A. M. Panich, R. M. Sardarly. Physical Properties of the Low-Dimensional A^3B^6 and $\text{A}^3\text{B}^3\text{C}^3_6$ Compounds, Nova Science Publishers, New York, USA, 2010.
- [13] A.M. Panich. Electronic properties and phase transitions in low-dimensional semiconductors, J. Physics: Condensed Matter 20 (2008) 293202. <https://doi.org/10.1088/0953-8984/20/29/293202>.
- [14] A.M. Panich, D. Mogilyansky, R.M. Sardarly. Phase transitions and incommensurability in the layered semiconductor TlInS_2 —an NMR study, J. Phys.: Condens. Matter. 24 (2012) 135901. <https://doi.org/10.1088/0953-8984/24/13/135901>.
- [15] O.Z. Alekperov, A.I. Nadjafov. Dielectric anomalies in monoclinic TlInS_2 polytypes,

- Inorg Mater. 40 (2004) 1248–1251. <https://doi.org/10.1007/s10789-005-0055-7>.
- [16] <https://materialsproject.org/materials/mp-865274>
- [17] A.U. Sheleg, O.B. Plyushch, V.A. Aliev. X ray diffraction study of incommensurable phase in B-TlInS₂ crystals, Fiz. Tverd. Tela 36 (1994) 226-230.
- [18] N.A. Borovoï, Yu.P. Gololobov, A.N. Gorb, G.L. Isaenko. On the ferroelectric phase transition in polytypes of β TlInS₂ crystals, Phys. Solid State. 50 (2008) 1946–1950. <https://doi.org/10.1134/s1063783408100260>.
- [19] M. Açıkgöz, S. Kazan, F.A. Mikailov. Electron Paramagnetic Resonance (EPR) Investigations of Iron-Doped Ferroelectric Ternary Thallium Chalcogenides, Applied Spectroscopy Reviews. 44 (2009) 181–209. <https://doi.org/10.1080/05704920902717864>.
- [20] F.A. Mikailov, B.Z. Rameev, S. Kazan, F. Yıldız, B. Aktaş. Electron paramagnetic resonance investigation of Fe³⁺ doped TlInS₂ single crystal, Solid State Communications. 135 (2005)114–118. <https://doi.org/10.1016/j.ssc.2005.03.043>.
- [21] J.A. Weil, J.R. Bolton. Electron Paramagnetic Resonance: Elementary Theory and Practical Applications, second ed., Wiley, New Jersey, 2007
- [22] A. Abragam, B. Bleaney. Electron Paramagnetic Resonance of Transition Ions, Clarendon Press, Oxford, 1970
- [23] S. Stoll, A. Schweiger. EasySpin, a comprehensive software package for spectral simulation and analysis in EPR, Journal of Magnetic Resonance. 178 (2006) 42–55. <https://doi.org/10.1016/j.jmr.2005.08.013>.
- [24] R.M. Sardarly, O.A. Samedov, A.I. Nadzhafov, I.Sh. Sadykhov. The influence of cation impurities on phase transitions in the TlInS₂ compound, Phys. Solid State. 45 (2003) 1137–1140. <https://doi.org/10.1134/1.1583804>.
- [25] S.F.A. Kettle. Symmetry and Structure: Readable Group Theory for Chemists, third ed., Wiley, Chichester, 2007
- [26] <https://easyspin.org/easyspin/documentation/frames.html>